STUDY OF IONOSPHERIC EFFECTS ON HF OTH RADAR USING COMPUTERISED RAY TRACING METHODS

A Thesis Submitted
In Partial Fulfilment of the Requirements
for the Degree of
MASTER OF TECHNOLOGY

By
SQN. LDR. PREM DATT BADONI

to the

DEPARTMENT OF ELECTRICAL ENGINEERING
INDIAN INSTITUTE OF TECHNOLOGY KANPUR
AUGUST, 1976

CERTIFICATE

Certified that this work 'Study of Ionospheric Effects on HF O.T.H. Radar Using Computerised Ray Tracing Methods' by Sqn. Ldr. P.D. Badoni has been carried out under my supervision and that this has not been submitted elsewhere for a degree.

N C Mathur

Dr. N.C. MATHUR
Professor
Department of Electrical Engineering
Indian Institute of Technology
KANPUR

August, 1976

ACKNOWLEDGEMENT

I am indebted to my thesis supervisor, Professor N.C. Mathur, for his continuous guidance and encouragement throughout this study. I wish to express my sincere thanks to him for his valuable suggestions.

Thanks are also due to Mr. S. Kapoor of the Computer Centre and my friend Mr. Bhartendu Gairola for their valuable help. Finally, Mr. J.S. Rawat deserves special mention for his excellent and neat typing work.

P.D. BADONI
(Sqn. Ldr.)

ABSTRACT

The High Frequency Over-the-Horizon (HF O.T.H.) Radar increases the ground range of conventional microwave radar from few hundred kilometer to few thousand kilometer in single hop. The OTH radar theory and the computed, results for mid-latitude ionosphere in respect of ground range, absorption, doppler shift and group-path changes, have been discussed. The computations were made on IBM 7044 computer using three - dimensional ray tracing program. The electron density and collision frequency are in tabular model. The values of electron density have been taken for mid-latitude locations from values quoted in the literature. The irregularity moves in north-south direction and has a gaussian distribution of electron density with a maximum at the centre. The simulation results show that maximum single hop range at 19 MHz is 3653 Km and the doppler shift is less than 1 Hz. The ionospheric absorption varies with solar activity and diurnal changes. It decreases with the increase of the frequency of transmission. The variations are from 4 to 19.1 db for high solar activity day, 6.4 to 37.1 db for low solar activity day and 1.4 to 8.4 db for night. The expected error in group-path due to irregularity in E region is less than 50 Km for a ground range not exceeding 3000 Km.

TABLE OF CONTENTS

		Page
CHAPTER 1	INTRODUCTION	1
	1.1 General	1
	1.2 Utility of HF O.T.H. Radar	3
	1.3 Scope	4
CHAPTER 2	OVER THE HORIZON HF RADAR	7
	2.1 Introduction	7
	2.2 Radar Range Equation of O.T.H. Radar	10
	2.2.1 F_p; Factor to account for Propogation effect.	11
	2.2.2 T_c; Coherent Processing time	12
	2.2.3 N_o; Noise Power per unit Bandwidth.	13
	2.3 Capabilities of O.T.H. Radar	14
	2.4 Applications	15
	2.5 Factors Affecting the O.T.H. Radar Operation.	17
CHAPTER 3	THE INFLUENCE OF THE IONOSPHERE	19
	3.1 Ionospheric Structure	19
	3.1.1 Refractive Index	19
	3.1.2 Phase Velocity	21
	3.1.3 Group Velocity	22

		Page
	3.2 Oblique Ray Paths	24
	3.2.1 Phase Path and Ground Range	24
	3.2.2 Group Path	26
	3.3 Attenuation of Radar Signal	27
	3.3.1 Ionospheric absorption	28
	3.4 Ionospheric Irregularities	31
	3.5 Ionospheric Doppler Shift	33
	3.6 Ionospheric dependence of Radar frequency	38
CHAPTER 4	ESTIMATION OF IONOSPHERIC EFFECTS	39
	4.1 Introduction	39
	4.2 General Description of Program	40
	4.2.1 Ionospheric Electron Density Model	43
	4.2.2 Ionospheric Irregularity Model	47
	4.2.3 Collission Frequency Model and data	49
	4.3 Radar ray path results	52
	4.3.1 Radar Frequency and Range	53
	4.3.2 Ionospheric absorption results	62
	4.3.3 Ionospheric doppler shift	64
CHAPTER 5	CONCLUSIONS	70
	REFERENCES	73

CHAPTER 1

INTRODUCTION

1.1 General:

RADAR stands for "Radio Detection and Ranging". The advances in Radar technology have been due to the rapid - growth of the : problem areas to which Radar is being applied. The military need for long range all-weather sensor of enemy aircraft gave initial push to the radar development. To day Radar has become a necessary and important aid, for Air/Sea/Land transportation network, Meteorological forecasting, understanding of earths atmosphere, the moon and the planets. The current capabilities of Radar technology, and the spectrum of applications are far too many. Though the vast majority of Radars, in the world, are known to operate at UHF or higher frequencies, there have been significant applications in the HF band.

The HF Radar is commonly referred as over-the Horizen (OTH) radar in the available open literature. O.T.H. radar technique makes possible, target detection upto the ranges of hundreds to thousands of kilometers. This is achieved by use of skywave propogation utilizing refraction through

ionosphere. To-day evidence exists of availability of necessary techniques and highly sophisticated equipment in use with some of the Western Countries at HF. Apart from powerful HF transmitter and sensitive directional receiver OTH Radar requires doppler processing for detection of targets in the presence of ground/sea clutter. Good ionospheric reflection without much absorption aids in detection at greater ranges. Since the ionospheric election density is variable we need different frequencies for different ranges or time of day/year or sunspot cycle. This requirement is met with a secondary vertically sounding radar and computer to calculate optimum frequencies on real time scale, OTH Radar transmitter and receiver are then tuned on to these frequencies to obtain desired range.

The OTH Radar requires a massive antenna structure for desired narrow beam width in horizental plane. The antenna of OTH Radar is required to be installed on good conductivity ground plane, extending some 3 Km, in the forward direction. Clarke[6] has shown that the use of Aperture - synthesis technique can reduce the size of OTH Radar Antenna and also can improve the accuracies in measurements. The secret of popularity, of OTH Radar in recent years inspite of high cost of manufacture and development, lies in its utility in different fields.

1.2 Utility of OTH Radar [6,12,22]:

Radar is one of the techniques for remote sensing. Other electromagnetic techniques include optical sensors such as telescopes, electrooptical sensors such as television and sensors of infra-red or thermal radiations from bodies. Radar is unique among electromagnetic sensors because it is an active sensor; the signal it receives is the one generated by its own transmitter. Thus, we see in OTH Radar a unique and powerful all weather sensor which can extend the detection range of targets to many thousands kilometers. Briefly we can say that the HF OTH radar is utilized for following purposes:

i) Detection of targets in the regions where LOS radar can not be installed such as sea or unfriendly territory. These target are usually aircraft, missiles or ships.

ii) Sensing sea state such as the height of waves.

iii) Gathering information about land.

iv) Exploration of earths atmosphere.

The development and manufacturing cost of OTH is quite high, but the utilities outweigh its cost in host of applications. Our aim in this work is to study the

propogation aspect, of OTH waves, which is most important. In order to make OTH Radar a reliable aid in its utilization we should have complete, knowledge of the effects of the propogation media on its performance.

1.3 Scope:

OTH Radar uses sky-wave propogation via ionosphere for electromagnetic energy path from Radar Transmitter to the receiver. Thus the Radar beam illuminates large area of surface of earth. The ground or sea return signal is large compared to the external noise level or target echo. To extract the useful information about the target, we need to employ doppler processing. The transmitter power should be such that the system engineering is cost-effective. Therefore we should know the absorbtion introduced by the ionospheric path. Also the irregularities in ionosphere introduce a doppler shift in the OTH echo. A knowledge of this doppler shift is necessary to decide the doppler filter bandwidth for OTH Radar which always uses doppler signal processing.

In this thesis, an attempt is made to calculate the ionospheric path absorption and doppler shift due to movement of irregularities. For this purpose we use ray

tracing technique. The calculation which would have been otherwise quite difficult to make have been done with the help of Ray tracing. Program [14,15]. This program has been modified for use on IBM 7040 with the inclusion of differential equations for absorption and doppler shift. The calculations have been made without the inclusion of magnetic field throughout this work. The calculations of ionospheric absorption, which is due to collisions and depends on the refractive index of the ionosphere has been given realistic approach by including the experimental values of electron density, obtained by various scientist for mid latitudes. This is done by incorporating a tabular profile of electron density and collision frequency. The values have been calculated for different time of day and for different solar(cycle) activity. This is helpful to OTH Radar designer to cater for diurnal, and solar cycle changes in the ionosphere.

To calculate the ionospheric doppler shift an irregularity with eliptical cross-section with only North-South movement has been introduced. The dimensions of the irregularity have been assumed in the range of observed values for Indian sub-continent. The variation of the refractive index due to irregularity is assumed to be

Gaussian in nature [14,15] with a variation of1-10 percent. The maximum being at the centre of irregularity.

The present study has been devided in four parts. In chapter 2 we discuss the various aspects of OTH radar along with its' special features compared to micro-wave radars. Chapter 3 gives the influence of ionosphere, on the OTH Radar, pertaining to the parameters of our interest such as effect of frequency on range, absorption of signal and doppler shift due to the irregularities. The ionospheric effects have been evaluated with the ray-tracing digital computer program in chapter 4. The conclusions drawn as a result of this simulation are summarised in chapter 5.

CHAPTER 2

OVER THE HORIZEN HF RADAR

2.1 Introduction:

Modern radar, an active sensor of varieties of targets of interest, are widely used for military, civilian and scientific applications. Majority of them operate at UHF and microwave frequencies. It is of interest to note that the development of Radar started in HF spectrum. Marconi recognised the potentialities of radio wave detection and strongly urged their use. First pulsed Radar at HF was employed by Breit and Tuve in 1925 for measurement of the height of ionosphere. The first operational Radar for aircraft detection was also at HF.

The development and manufacture of radar at HF frequency just before world war II and during world war II was because of compulsion as the other component required for use in radar equipment had not been developed till then. Because of various difficulties, in HF region such as crowded spectrum, limited band width, high ambient noise and wide beam widths, radar manufacturers switched over to UHF and microwave frequencies for radar development during and the inter-world-war period itself[12,22]. However people in this

field were aware of the important properly of HF radiation to propogate beyond the horizon. The propogations beyond the horizon is firstly by ground waves differacted around the curvature of the earth or secondly by sky waves refracted by the ionosphere. The range of ground wave HF radar may be 200-400 Km. where as that of HF sky wave radar know as OTH radar may be 1000 Km to 4000 Km and even more. Thus we see OTH extends the LOS range to 10 times which is a great advantage from military and and civilian application point of view. Now the changes in inaccessable territorial sea, ground and sky can be sensed and used advantageously without the knowledge of the country to which they belong to.

The development of OTH radar was started by Naval Research Laboratory in early 1950. The information given here is the one available in the western open literature. The intricate details of developments may still be secret. The OTH Radar signal strength at the receiver from targets may be very small compared to the extremely large ground or

sea clutters. Depending upon the antenna beamwidth and transmitter pulse width, the clutter echo may be as large as 80 db compared to the aircraft return echo. Extraction of the target information from the OTH Radar echo requires sophisticated signal processing techniques which have been developed over the last few years. Extraction of useful information requires firstly high target to clutter ratio secondly low minimum detectable signal. This all means high resolution in doppler and azimuth. Doppler processing is necessary to recognise the target echo from moving clutter and external noise. High resolution in range means large receiver band-width or say small pulse width of radar transmitter. In case of OTH Radar which uses a dispersive medium like ionosphere for propogation, we can only have a maximum bandwidth of 100 KHz. This corresponds to a range resolution of 1.5 Km (maximum) Azimuth resolution of 1° means that an antenna of 2 Km size in horizontal direction is required which is a massive structure. The use of synthetic aperture antenna has also been reported for high angle resolution.

Naval Research Laboratory experiments have shown that one way sky wave path of Radar signal have been found stable for the order of seconds. Hence coherent radar detection of targets is possible. Improvements in signal

processing such as use of ferrite-core memory devices and digital processing have increased the reliability of OTH. Three OTH radar installation viz. NRL Madrie OTH radar at Chesa- Peake Bay-field Virginia, Rock Bank near Melborne, Australia and Orford Ness on the Suffolk Coast have been reported by Peter Laurie [18].

2.2 Radar Range Equation of OTH Radar [12]:

Radar Range Equation gives us an insight into the problems and characteristics of HF OTH radar. The commonly used radar range equation is

$$R_{max.}^4 = \frac{P_{av}\, G_t\, G_r\, \lambda^2\, \sigma\, F_p\, T_c}{(4\pi)^3\, N_o\, (S/N)\, L_s} \qquad (2.1)$$

where

$R_{max.}$ maximum range

P_{av} average power of Radar

G_t Transmitting antenna gain

G_r Receiving antenna gain

λ Transmitted signal wavelength.

σ target cross section

F_p factor to account for propogation effects

T_c coherent processing time

N_o noise power per unit bandwidth

(S/N) signal to noise ratio required for detection

L_s system losses

It is quite clear from (2.1) that for long range detection, we should have high average power output & high antenna gains. These factors are quite common for all radars irrespective of their frequency of operation. HF OTH Radar differs in Radar Range equation from other conventional (UHF & microwave) Radar due to the inclusion of following factors:

(a) F_p: Factor to account for propogation effects.

(b) T_c: Coherent processing time.

(c) N_o: Noise power per unit bandwidth.

A detailed discussion of these factors is given below to gain insight into the significance of these factors.

2.2.1 F_p: Factor to Account for Propogation Effects:- Conventional microwave line of sight (LOS) radar signal undergoes path losses but these path losses are quite different than the path losses included in factor F_p for HF OTH Radar. OTH path is through ionosphere which has a statistical nature. Therefore this path loss we shall call as ionospheric path loss which is also statistical in nature and keeps on changing

with time and location of transmission. Secondly path loss includes the loss due to polarisation mismatch Polarisation mismatch may occur in case of LOS microwave radar during heavy rain or hail storm. This can be elimenated by transmitting circularly polarised waves during that period. In case of OTH Radar, where the propogation is through refracting medium, we always have the polarisation mismatch which has to be accounted for by including polarisation mismatch factor. Thirdly the refracting nature of the ionospheric path introduces focusing and defocusing of the radar rays. This results in the decrease or increase in the signal strength at a particular place. Thus we have focusing gain or loss in the OTH Radar path. All these three factors make OTH radar unique in respect of factor F_p.

2.2.2 T_c: Coherent Processing Time [12,22]:- The number of pulses, n_B, returned from a point target as the antenna scans through its bandwidth θ_B degrees is

$$n_B = \frac{\theta_B \, f_r}{6 \, W_m}$$

where f_r is pulse repetition frequency in C/S W_m is antenna scan rate, rpm. We can say that n_B is number of pulses integrated in one scan time from a point target or some times is also called number of hits integrated. Coherent processing time T_c is defined mathematically as

$$T_c = \frac{n_B}{f_r}$$

T_c indicates the dwell time of doppler radar that gives a doppler frequency resolution of $\frac{1}{T_c}$ Hz. Also the ionospheric path of radar signal should be stable for at least this period, otherwise the doppler shift introduced by the ionospheric path itself will reduce the signal strength at the receiver and also reduce the resolution of targets in doppler.

2.2.3 N_o; The Noise Power/Unit Bandwidth :- At HF the ambient noise level is high and the receiver sensitivity is limited by the external noise which enters the radar receiver along with the signal. At microwave frequencies the ambient noise level is low and receiver sensitivity is mainly determined by internal noise level. The factor N_o at HF spectrum is made of following factors:

(a) Cosmic noise.

(b) Atmospheric Absorption Noise .

(c) Atmospheric and man made noise.

These factors are usually negligible at microwave frequencies and as such inclusion of them in HF OTH Radar equation makes them unique.

2.3 Capabilities of OTH Radar[12,18]:

The targets of interest of HF OTH Radar are same as that of microwave radar. The performance figures given below give us insight into the capabilities of an HF OTH Radar. These figures are nominal and can be achieved with proper design and installation of OTH Radar.

2.3.1 Range Coverage: The single hop range could be from 1000 Km to 4000 Km. The longer ranges can be achieved with multi-hop propogation but the performance quality becomes poorer as the number of hops increase.

2.3.2 Azimuthal Coverage: HF OTH Radar can be made with 360° coverage but normally it is preferred to scan the limited area of interest. The radar coverage of 60° to 120° is reported more common.

2.3.3 Targets: The targets of interest are aircraft, ships; missiles, nuclear explosions , prominant surface features such as mountains, cities and island ,sea, satellites below the highest ionisation density layerof ionosphere, meteors and aurora.

2.3.4 Range Resolution and Accuracy: This can be as low as 2 Km. but typical common figures are 20-40 Km. The range accuracy is of two types. Firstly relative range accuracy

which is 2-4 Km for a target location relative to a known location observed by the same radar. Secondly we have absolute range accuracy which is 10-20 Km, with good real time ionospheric path assessment.

2.3.5 Angle Resolution: Angle resolution depends on the beam-width of the radar antenna radiation pattern. It can be as fine as 1°. It means that targets separated by 50 KM at 3000 Km range can be seen separated.

2.3.6 Doppler Resolution: The targets whose doppler frequencies differ by .1 Hz or so have been found to be resolved. This is done by putting the doppler filters of .1 Hz bandwidth.in receiver.

2.4 Applications:

The OTH Radar has increased the maximum radar range by an order of magnitude. Thus we are able to detect, observe and track the targets beyond the line of site range in places which are inaccessable with conventional microwave radar. The examples of these are dection over the sea and hostile territory. The application of HF radar can be divided in three major headings as following:

(a) Detection and Control

(b) Ionospheric Studies

(c) Sensing of sea and ground surface changes

2.4.1 Detection and Control: The OTH Radar with its range from 1000-4000 Km can observe vast space and surface. The objects like aircraft, missile, nuclear explosion and ships movements can be detected. Successful tests have been carried out for detection and control of aircraft accross Atlantic Ocean. Thus with OTH Radar, we can improve the safety of the air and sea traffic. The detection of nuclear explosions and missiles adds another advantage to the credit of OTH Radar which could not have been done so precisely with any other system.

2.4.2 Ionospheric Studies: This is the field which the applicati of HF Radar has been reported long time back. OTH Radar can explore the atmosphere of inaccessable Geographical locations at oblique incidence. The facts they found out can be utilized advantageously for various other uses.

2.4.3 Sensing of Sea and Ground Surface changes: The OTH Radar doppler frequency spectrum of sea and ground clutters is very small compared to the doppler frequency of aircraft, ship or missile targets. Therefore in OTH detection we put a narrow doppler filter to separate the aircraft or ship radar echos from the ground and sea clutter. The ground and sea clutter signal is then analysed to find out

surface conditionss and the wind velocity along with their direction over sea. Similarly from ground clutter we can deduce the change and type of the surface like mountain or forests etc.

2.5 Factors Effecting the O.T.H. Radar operation:

OTH radar utilizes frequency spectrum from 2 MHz to 30 MHz. At the lower edge of the frequency spectrum, number of problems are encountered like decrease in radar cross section of the target. Further HF propogation is with sky wave through ionosphere. Ionospheric path is statistical in nature and has dynamic irregularities. Thus following detrimental factors exist for operation of HF OTH.

a) Multipath interference results in fading of signals at times.

b) Additional losses are introduced due to ionospheric absorption.

c) Motions inherent in ionosphere like irregularities can limit the accuracy of angle or resolution and doppler resolution.

d) Low PRF is used to avoid ambiguities in range but it introduces ambiguities in doppler.

e) Magnetoionic path of transmission introduces polarisation fading.

f) Dynamic nature of ionosphere allows only a particular area to be illuminated at a particular time. Hence real time sensing of atmosphere and selection of frequency is required.

g) The HF frequency spectrum is quite congested and other user interference is expected.

h) Since the area illuminated at ranges like 3000 Km or so is quite large we get large ground clutter which make detection difficult.

i) Difficult design of large antenna.

In order to over come the difficulties certain compromises are made for optimum operational effeciency. Some of the difficulties are over come by increasing the design complexities. This increases the cost of the HF installation but the utilities out weigh the cost.

CHAPTER 3

THE INFLUENCE OF IONOSPHERE

3.1 Ionospheric Structure[4,7,8]

The ionosphere is the ionised medium in the earth's atmosphere, lying between 50 Km and about one earth radius. The electron density of the ionosphere varies with height and thereby influences the radio wave propogation through it. The ionosphere is devided in D, E and F regions. Different layers of electron density exist within the regions. The critical frequency and electron density of the layers are important parameters from the point of view of radio propogation in HF.

3.1.1 Refractive Index: Ionosphere is a refracting medium whose refractive index n is given by Appleton-Hartee Formula[4] as

$$n^2 = 1 - \frac{X}{1-jZ-\frac{Y_T^2}{2(1-X-jZ)} \pm \left(\frac{Y_T^4}{4(1-X-jZ)^2} + Y_L^2\right)^{\frac{1}{2}}} \qquad (3.1)$$

Where

n = complex refractive index of ionosphere.

$$X \triangleq \frac{Ne^2}{\epsilon_o mW^2} = \frac{W_N^2}{W^2}$$

$$W_N = \frac{Ne^2}{\epsilon_o m} = 2\pi f_N \; ; \quad W = 2\pi f$$

N = electron density

e = charge of an electron

m = mass of an electron

ϵ_o = permitivity of free-space

W_N = angular plasma frequency

W = angular frequency of radio-wave

If f is in MHz and N in electron/cm^3 then

$$X = \frac{80.61N}{f^2} \times 10^{-6}$$

$Y_L \triangleq \frac{e\,BL}{mW}$ due to longitudinal component of imposed magnetic field.

$Y_T \triangleq \frac{e\,B_T}{mW}$ due to Transverse component of imposed magnetic field.

$Z = \frac{\nu}{W} =$ Ratio of collisin frequency to the angular frequency of radio-wave

For the sake of simplicity we neglect the effect of earth's magnetic field. Therefore substituting $Y_L = Y_T = 0$ in (3.1) we get

$$n^2 = 1 - \frac{X}{1 - jZ} \tag{3.2}$$

Let μ be the real part of phase refractive index n and x be the imaginary part of it then we have

$$n^2 = (\mu - jx)^2 = 1 - \frac{X}{1-jZ}$$

$$= \mu^2 - 2j\mu x - x^2 = 1 - \frac{X}{1+Z^2} - \frac{jXZ}{1+Z^2} \tag{3.3}$$

Comparing real and imaginary part of both sides of (3.3) we get

$$x = \frac{1}{2\mu} \cdot \frac{XZ}{1+ Z^2} \tag{3.4}$$

3.1.2 Phase Velocity: The phase velocity of radio-wave through ionosphere of refractive index n is defined as

$$v = \frac{C}{n}$$

If magnitic field is neglected then

$$v = C \left(1 - \frac{X}{1 - jZ}\right)^{-1/2} \tag{3.5}$$

If collisions are also neglected then the phase velocity is given by the relation.

$$v = C \left(1 - \frac{Ne^2}{m \epsilon_o w^2} \right)^{-1/2} \qquad (3.6)$$

3.1.2 Group Velocity[8]: Group velocity is the velocity of propogation of envelope of the radio wave in ionospheric media whose propogation constant k is varying with the frequency of wave. Mathematically we can define it as

$$u = \frac{\delta w}{\delta k} \qquad (3.6a)$$

where u = Group Velocity.

In the limit as $\delta w \rightarrow 0$ and $\delta k \rightarrow 0$ we obtain

$u = \left(\frac{dw}{dk}\right)_{k_o}$ where k_o is the value of propogation constant at which $\frac{dw}{dk}$ has been evaluated.

We can now define group refractive index as

$$= \frac{C}{u} \qquad (3.7)$$

$$= C \frac{dk}{dw} = C \frac{d}{dw} (\mu w)$$

$$= \mu + w \frac{d\mu}{dw}$$

$$= \mu + f \frac{d\mu}{df} \qquad (3.8)$$

In case the magnetic field is not considered then substituting

$$\mu = \left(1 - \frac{f_N^2}{f^2}\right)^{1/2} \quad \text{in (3.8)}$$

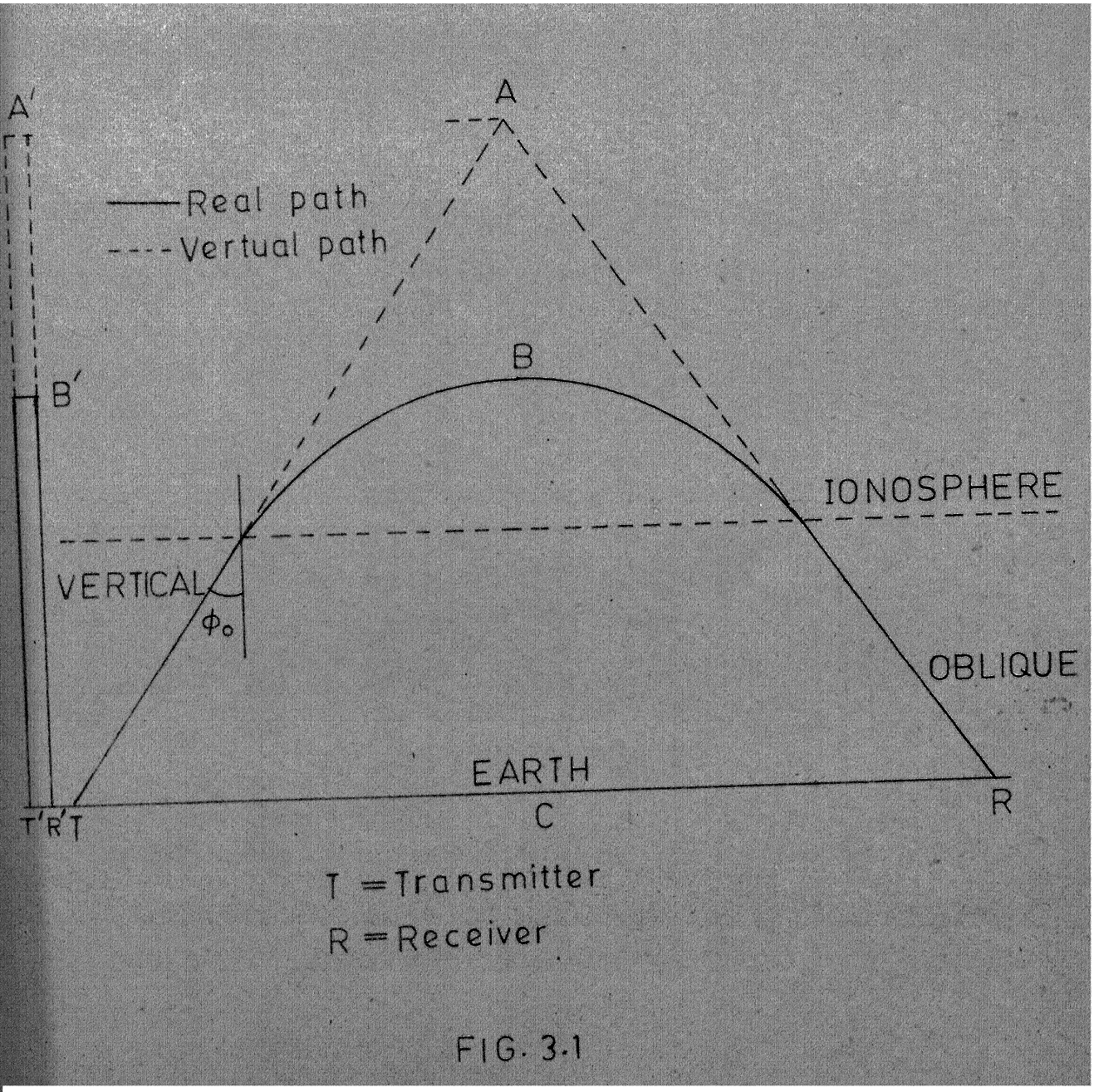
A'
A
Real path
Vertual path
B'
B
IONOSPHERE
VERTICAL
ϕ_0
OBLIQUE
EARTH
T'
R'
T
C
R
T = Transmitter
R = Receiver

FIG. 3.1

We have

$$\mu' = \frac{d}{df}(\mu f) = \frac{1}{\mu} \qquad (3.9)$$

3.2 Oblique Ray Path [8]

The secant law for a wave entering the ionosphere with an angle ϕ_o (figure 3.1) is as given by

$$f = f_v \sec \phi_o \qquad (3.10)$$

where

f is frequency of an oblique ray reflacted from a height.h.

f_v is vertical incidence frequency which is reflected from the same height h. (3.10) shows that ionosphere can reflect much higher frequencies at oblique incidence than at vertical incidence.

3.2.1 Phase Path and Ground Range [9,10,17]: The phase path P is defined as

$$P \triangleq \int_T^R \mu \, dS \qquad (3.11)$$

Where dS is an element of distance along the ray path (Fig. 3.2).

The ground range R is defined (Fig. 3.2,& Fig. 3.3)

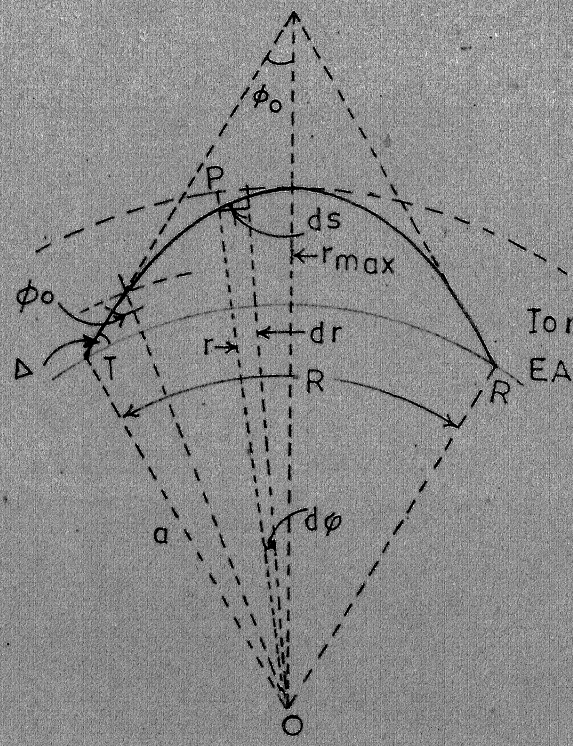

FIG. 3-2

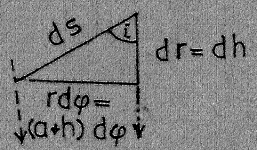

To center of the eart

FIG. 3-3

$$R = a \int_{T}^{R} d\phi \qquad (3.12)$$

Where

R = The ground range

a = Radius of Earth

$d\phi$ = Angle subtended by dS at the centre of earth.

It can be shown that ground range and phase path are related by [10]

$$\frac{\partial P}{\partial \Delta} = \cos\Delta \frac{\partial R}{\partial \Delta} \qquad (3.13)$$

3.2.2 Group Path: The group path P' is defined as

$$P' = \int_{T}^{R} \mu' dS$$

Where μ' is the group refractive index. It can be shown that [10]

$$R \leq P' \cos\Delta \leq \frac{(a + h_m)^2}{a^2} R \qquad (3.14)$$

where

Δ = angle of elevation of the ray at the transmitter.

h_m = height of maximum ionisation.

From (3.14) it is evident that $R \propto P'$ and an error in group-path means the error in ground range.

Also group path and phase path are related by [17]

$$\frac{dP}{df} = \frac{1}{f} \left(P' - P \right) \qquad (3.15)$$

The above relation holds good for any profile.

3.3 Attenuation of Radar Signal [7,8]:

The radar signal suffers attenuation due to following factors while travelling from Radar transmitter to the Receiver:

(a) Ohmic loss in the transmission and reception line and their respective antennas.

(b) Polarisation mismatch loss of the receiving and transmitting antennas.

(c) Path loss.

(d) Antenna aperture loss.

While dealing with the propogation of radar signal at HF we shall be interested in a portion of path loss which can be measured and accounted for while designing the Radar. The path loss suffered by HF radar signal in propogation via ionospheric path is constituted of three factors viz.

i) Inverse distance loss (L_d), this is due to dispersion of energy in the medium.

ii) Absorption in the ionosphere denoted by L_a.

iii) Focusing or defocusing gain or loss denoted by L_f,

L_p = The propogation path loss is then given by

$$L_p = L_a + L_d + L_f \qquad (3.16)$$

We shall now describe (L_a) the ionospheric absorption loss suffered by radar signal in detail.

3.3.1 Ionospheric Absorption [7,8]: The electric vector of travelling radio wave sets the electrons(or ions) in the ionosphere into motion. These electrons collide with other particles in the plasma and the energy is lost in the form of thermal energy. The energy lost is taken from the radio wave and thus causes absorption of radio wave. The electron density is low in 'D' region and the collision frequency is high compared to the E and F regions. High collision frequency of 'D' region results into higher absorption. Also we know that lower the frequency of propogating radio wave higher is the absorption since it spends more time in high collision frequency region.

From equation (3.4) we have imaginery part of refractive index

$$x = \frac{1}{2\mu} \quad \frac{XZ}{1+Z^2}$$

The equation of a wave travelling in X direction is given by

$$E = Eo \exp i\left(wt - \frac{w}{C} n x1 \right) \qquad (1.17)$$

but $n = \mu - ix$ and therefore we have

$$E = Eo \exp\left(-x \frac{w}{C} x1\right) \exp i\left(wt - \frac{w}{C} \mu x1\right) \qquad (3.18)$$

(3.18) is a wave whose amplitude is decreasing exponentially with distance X1 travelled by it. The quantity $x \frac{w}{C}$ is the measure of amplitude decrease and is called Absorption Coefficient L.

$$L = \frac{w}{C} x \qquad (3.19)$$

Substituting the value of x i.e. immaginery part of refractive index from (3.4) in (3.19) we get

$$L = \frac{e^2}{2 \epsilon_o mC} \cdot \frac{1}{\mu} \cdot \frac{N \nu}{W^2 + \nu^2} \qquad (3.20)$$

where L is in nepers, ν is the collision frequency in Hz.

Absorption in (3.20) can be devided into two types:

i) Non-deviative absorption which occurs mostly in the region where $\mu = 1$ and $N\nu$ is large. This takes place mostly in 'D' region of the ionosphere.

ii) Deviative absorption , which occurs near the top of the trajectory or any where along the path where bending is more.

Now substituting the values of e, m & C, we get absorption coefficient as given below:

$$L = 5.3 \times 10^{-6} \quad \frac{1}{\mu} \frac{N\nu}{w^2+\nu^2} \quad N_p/m$$

$$= 4.6 \times 10^{-2} \quad \frac{N\nu}{w^2+\nu^2} \quad db/Km. \qquad (3.21)$$

where N is electron/cm^3

ν is Hz/sec.

L is some times called absorption index. Total absorption can be obtained by integrating L over the ray path from transmitter to receiver. L_a the total absorption in the absence of magnetic field is given by

$$L_a = \int_S L\,ds \qquad (3.22)$$

$$= \int_S \frac{0.046}{\mu} \cdot \frac{N\nu}{w^2+\nu^2} \, ds \qquad (3.23)$$

But $P' = \int \mu' ds$

$ds = \frac{dP'}{\mu'}$

Hence

$$L_a = \int_{P'} \frac{0.046}{\mu\mu'} \cdot \frac{N\nu}{w^2+\nu^2} \, dP' \qquad (3.24)$$

(3.24) gives the total absorption of radio wave along the group path P.

3.4 Ionospheric Irregularities [18,23,to 26]:

The ionisation irregularities are present in the ionosphere during day and night hours. The irregularities are more in number during day time compared to night [25]. The causes of these irregularities may be the travelling disturbence in the ionosphere [26] or cross field instabilities and wind shears [19]. The studies of ionisation irregularities have been greatly facilitated with the availability of artificial satellite. The radio signal received from the satellite show regular and slow fading rate normally, however, when the radio ray passes through the irregularity, it causes, the fluctuations in the fading rate. The duration of this fluctuation depends on the horizontal size of the irregularity, while the amplitude variations give the rate of change of electron content in the irregularity.[26]

The irregularities in E and F regions of Indian sub-centiment have been studied in past decade with the help of satellite explorer-22 at Delhi[27] and with Rocket borne probe/VHF back-scatter radar at Thumba[19]. The irregularities thus studied may be classified in two categories viz. Large scale irregularities and small scale irregularities. The

small scale irregularities have been found to be field aligned along the earth's n magnetic field while the large scale irregularities are not field aligned.[27] The large scale irregularities have been reported to have a size of 10-400 Km with heights from 160 to 600 Km and without any evidence of diurnal variations. The electron content has been found to be proportional to the number of irregularities present and to their size. The large scale irregularities were also found to have an axial ratio of the horizontal to vertical size of the order of 10:4. The horizontal velocity of irregularities in 'F' region have been reported 500 Km/ min generally[25] .

For our present work we need to know the irregularitie in their size, shape and velocity. The E region has been studied by Satya Prakash et.al [19] over Thumba. Their studies have indicated three types of irregularities present in the ionosphere over the equitional region viz. (i) Large scale irregularity type L; These irregularities are in between the heights of 90 to 125 Km with more than 40 Km size in horizontal and few Km is vertical. During the occurance of such disturbences the electron density varied by a factor of 4 to 25. (ii) Type M: These have a scale size of 30 to 300 meters. These are in the height range of 80 to 140 Km. (iii) Type S: These are

1 to 5 meter in scale size and they occur in the height region of type M but with smaller amplitudes.

Some other workers who studied the large scale irregularities in India have reported the scale sizes of 80-120 Km. with the horizontal speed of morement between 60 to 180 Km/sec[24]. The electron content varies, from .1 to 10 percent from that of the back-ground ionosphere, due to the presence of irregularity. The large scale irregularities have been attributed due to the propogation of a wave of disturbance through the ionosphere. The presence of irregularities in the radio wave path introduces group path changes and doppler shifts. The location of irregularity in path of radio ray decides the group path changes. Maximum change in group-path occurs when the irregularity is located at a height very near to the height of reflection of radio ray[17].

Based on the forgoing, and the apogee height which the radar ray reaches in an atmosphere free of irregularities, the suitable scale size and speed of movement of irregularity may be selected for finding the doppler shift.

3.5 Ionospheric Doppler Shift[8, 17]:

The instantaneous frequency shift is caused by the rate of change of phase-shift with time. This amounts

to changing the refractive index with time or moving of source of the energy (Transmitter) with respect to the observer (Receiver) during the propogation of radio waves. Thus the frequency shift caused due to the change of phase or say refractive index of the medium is called the Doppler shift and denoted by Δf

Let the phase of a wave be denoted by

$$\phi = w - K \cdot r \qquad (3.25)$$

Where w is angular frequency of transmission of the wave and K is propogation vector in the direction of phase propogation with amplitude $2\pi/\lambda \cdot r$ is the position of wave at time t. Therefore we see from (3.25) if K or γ change with time then it will mean ϕ varies with time and angular frequency will shift by Δw. The main causes of doppler frequency shift are the movement of irregularities in the ionosphere.

Let us consider a wave of frequency f sent from a transmitter and received at a receiver at a distance S. Let the phase of the wave at transmitter be zero then its phase at receiver will be (in radians)

$$\phi = 2\pi \int_S \frac{dS}{\lambda} = \frac{2\pi f}{C} \int_S \mu \, dS$$

But $\int_S \mu ds = P$ (the phase path)

$$\phi = \frac{2\pi f}{C} P \qquad (3.26a)$$

$$= \frac{w}{C} P$$

Normally only changes in ϕ can be measured so we put (3.26a) in the form

$$\Delta\phi = \frac{2\pi f}{C} \Delta P \qquad (3.26)$$

Mathematically doppler shift is now defined as

$$\Delta f \triangleq \frac{d}{dt} \left(\frac{\Delta \phi}{2\pi} \right)$$

$$= - \frac{f}{C} \frac{d}{dt} (\Delta P) = - \frac{\dot{\Delta P}}{\lambda} \qquad (3.27)$$

negative sign indicates that decrease in phase means positive frequency shift.

(3.27) can be written as

$$\frac{d(\Delta P)}{dt} = \frac{dP}{dt} = \frac{d}{dt} \int_S \mu \, ds = \frac{\partial \mu}{\partial t} ds$$

where S is ray path and μ is the real part of the phase refractive index. Substituting in (3.27) we get

$$\Delta f = - \frac{f}{C} \int_S \frac{\partial \mu}{\partial t} ds \qquad (3.28)$$

Neglecting the earth's megnetic field and collisions we have real part of refractive index from (3.18) $\mu = (1-X)^{1/2}$ and

$$\frac{\partial \mu}{\partial t} = -\frac{\partial X}{\partial t}\left(\frac{1}{2\mu}\right)$$

Thus

$$\Delta f = -\frac{K}{2\mu f c} \int_S \frac{\partial N}{\partial t}\, ds \qquad (3.29)$$

Where $K = 86.61 \times 10^{-6}$ for f is in MHz

and N is electrons/cm^3.

Now we can write

$$\frac{dN}{dt} = \frac{dN}{d\lambda} \cdot \frac{d\lambda}{dx} \cdot \frac{dx}{dt} \qquad (3.30)$$

where x is the distance, moved by the irregularity horizontally, known as longitudinal idisplacement of irregularity. λ is geomegnetic latitude of the centre of irregularity. Fig. 3.9a shows the projection of irregularity on a horizontal plane and defines the coordinate system. Fig. 3.9b is cross - section of irregularity in vertical plane.

For a direction of motion in the x-direction (southwards) the latitude decreases as the irregularity moves and $\frac{d\lambda}{dx} = -\frac{1}{r}$, where r = distance of the irregularity from the centre fo of the earth.

$$\frac{dN}{dt} = \left(-\frac{1}{r}\right)\frac{dN}{d\lambda} \cdot \frac{dx}{dt}$$

If we consider that the irregularity is moving north-south i.e. $\frac{dx}{dt}$ is velocity of Torus say denoted by V then we have

$$\frac{dN}{dt} = -\left(\frac{1}{r}\right)\frac{dN}{d\lambda} V \qquad (3.31)$$

Substituting (3.31) in (3.30) and $ds = \frac{dP'}{\mu'}$

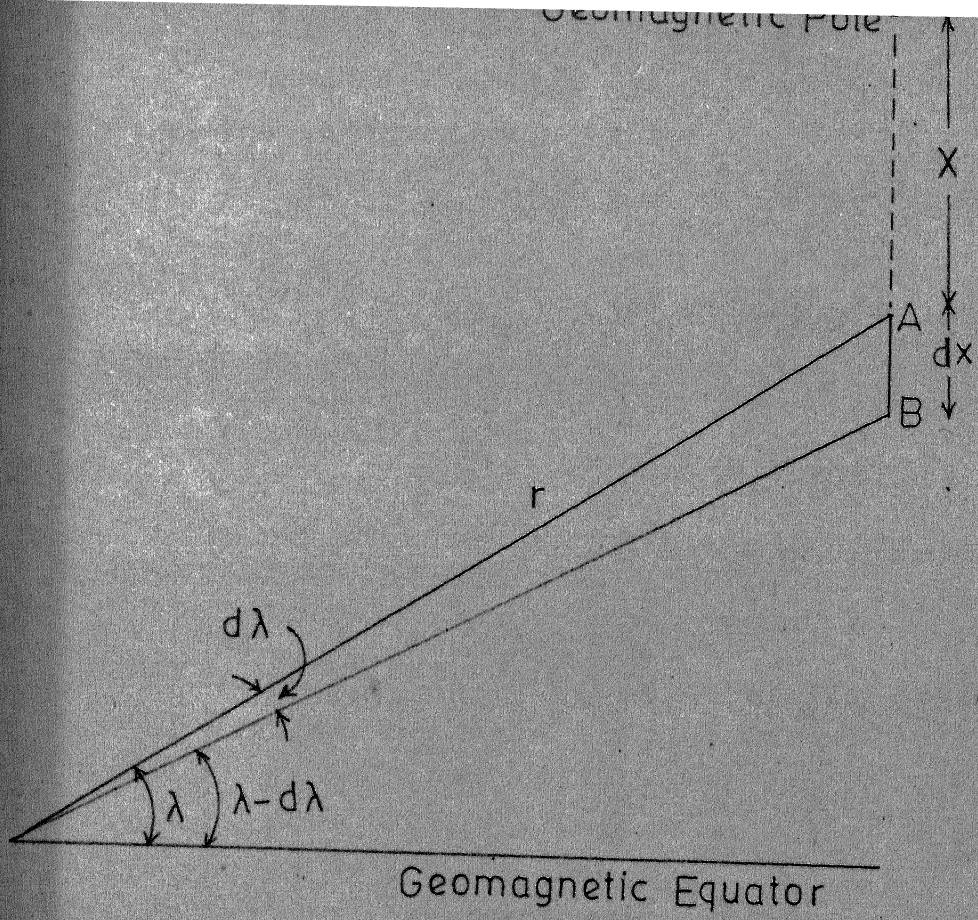

FIG.3·9 (a)

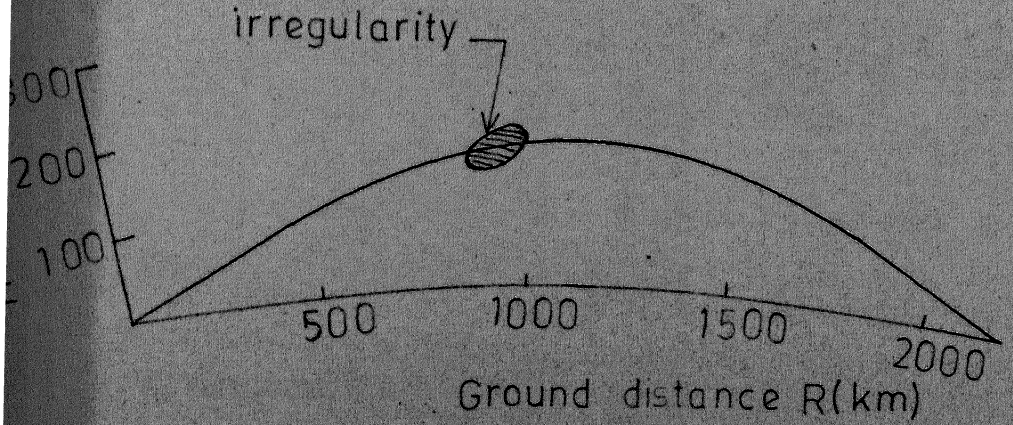

FIG·3·9 (b)

$$\Delta f = \frac{K}{2\mu\mu' fc} \int_{P'} -\left(\frac{1}{r}\right) \frac{dN}{d\lambda} V \, dP' \qquad (3.32)$$

In this $\frac{dN}{d\lambda}$ has to be obtained from irregularities electron density distribution model.

3.6.1 Ionospheric Dependence of Radio Frequency:

The Ionospheric absorption and doppler shift given below indicate the frequency dependence of these parameters.

$$\text{Absorption in dbs} = L_a = \int_{P'} \frac{0.046}{\mu\mu'} \cdot \frac{N\nu}{w^2+\nu^2} \, dP'$$

$$\text{Doppler shift} = \Delta f = \frac{K}{2\mu\mu' fc} \int_{P'} -\left(\frac{1}{r}\right) \frac{dN}{d\lambda} V \, dP'$$

Depending on the range requirement and available power output of the radar equipment we have to find a frequency which gives minimum absorption loss and doppler-shift. The low absorption helps in increasing the probability of detection where as low doppler shift improves the resolution in doppler. Therefore in Chapter 4 we discuss the results of our measurements of doppler shift and ionospheric absorption for the assumed models of ionosphere for different frequencies of propogation.

CHAPTER 4

"ESTIMATION OF IONOSPHERIC EFFECTS"

4.1 Introduction:

Ionosphere affects the propogation of radar signal in High frequency range (3-30 MHz). The ionospheric effects in the HF range are evaluated in this section for the hypothetical geographical area of Indian sub-continant. An attempt has been made to evaluate the effect of ionosphere at different frequencies and elevation angles of transmission on ground range, absorption loss and doppler- shift of radar signal.

The parameters of interest to the user of radar are ground range, range resolution, doppler resolution Azimuth Coverage and elevation coverage. These parameters depend on the frequency in use and type of the ionosphere available for transmission. In order to work-out the frequency requirement for the complete ground distance of interest (for example 1000 Km to 3000 Km) we need to know the range covered by a frequency with specified beam width and elevation angle of transmission. The requirement of power output can be worked out more realistically if the

ionospheric absorption is known. The doppler shift and change in group path give the idea of doppler measurement accuracy and the range measurement accuracy. Since the change in group-path, introduced by irregularity, is equal to the error in range measurement. All these ionospheric effects are estimated in subsequent sections, for the High solar activity, Low solar act. and day and night conditions to find the values for extreme conditions. The radar designed with these parameters would work for all other ionospheres.

4.2 General Description of Program[14,21]

For the purpose of estimating ionospheric effects reported in this thesis, a versatile digital computer ray tracing program [14,21] has been used. The memory requirement of the program is 14 K to 16K depending on the type of model used and number of sub-routines required. In order to simulate the realistic values of absorption, doppler shift and group-path, we have chosen the tabular models of electron density and collision frequency. Through out this work the effect of earth's magnetic field has been neglected (though the program has the provision for it).

The ray tracing program traces the path of a radio-wave through the ionosphere for given transmitter

Location (height above ground, latitude and longitude), frequency of wave and direction of its transmission (both elevation and azimuth), the receiver height above ground and maximum number of hops required.

The program uses six differential equations given by Haselgrove in 1954. The present equations are with respect to independent variable group path denoted by t. The original equations were with phase path as independent variable. The six basic equations are:

$$\frac{dr}{dt} = \frac{1}{\mu\,\mu'}\left(V_r - \mu\,\frac{\partial \mu}{\partial V_r}\right) \tag{4.1}$$

$$\frac{d\theta}{dt} = \frac{1}{\mu\,\mu' r}\left(V_\theta - \mu\,\frac{\partial \mu}{\partial V_\theta}\right) \tag{4.2}$$

$$\frac{d\phi}{dt} = \frac{1}{\mu\,\mu' r \sin\theta}\left(V_\phi - \mu\,\frac{\partial \mu}{\partial V_\phi}\right) \tag{4.3}$$

$$\frac{dV_r}{dt} = \frac{1}{\mu'}\,\frac{\partial \mu}{\partial r} + V_\theta\,\frac{d\theta}{dt} + V_\phi \sin\theta\,\frac{d\phi}{dt} \tag{4.4}$$

$$\frac{dV_\theta}{dt} = \frac{1}{r}\left(\frac{1}{\mu'}\,\frac{\partial \mu}{\partial \theta} - V_\theta\,\frac{dr}{dt} + V_\phi\, r \cos\theta\,\frac{d\phi}{dt}\right) \tag{4.5}$$

$$\frac{dV_\phi}{dt} = \frac{1}{r \sin\theta}\left(\frac{1}{\mu'}\,\frac{\partial \mu}{\partial \phi} - V_\phi \sin\theta\,\frac{dr}{dt} - r\,V_\phi \cos\theta\,\frac{d\theta}{dt}\right) \tag{4.6}$$

Where r, θ, ϕ are spherical polar coordinates of a point on the ray path, V_r, V_θ, and V_ϕ are the components of

wave normal direction in the r , θ , and ϕ directions, and μ and μ' are the phase and group refractive indices.

The names of various sub-routines used from Jones [15] program are as following:

i) RAYTRC is Main Program
ii) TRACE
iii) Back-up
iv) OUTPUT
v) REACH
vi) HASEL
vii) POLCAR
viii) CARPOL
ix) PRINT
x) PUNCH
xi) RCOORD
xii) RKAMSB
xiii) RINDEX
xiv) TORUS
xv) ELDENS
xvi) GAUSSL
xvii) TABLEZ

All the differential equations are incorporated in the sub-routine HASEL, The integration of first 3 basic differential equations (4.1,4.2,4.3) given above gives us r θ , ϕ the spherical polar coordinates of the ray point while integration of last 3 equations (4.4,4.5,4.6), gives us

the components of wave normal directions as the ray progresses in ionosphere, using group path in place of phase path as independent variable has two advantages. Firstly it speeds up the program by decreasing the step length in real path near reflection automatically and secondly it releives the error checking mechanism in the program from decreasing the step length to maintain accuracy. In addition, the program evaluates absorption and doppler shift. This is done by including the differential equation for them in sub-routines HASEL. The relative error in any single step of measurement is not more than one part in thousand. The program can have more accuracy but the cost of computations will be more.

4.2.1 Ionospheric Electron Density Model: The electron density of the ionosphere is a function of the time of the day, season of the year, geographical location of place and sun-spot number. In view of choosing a realistic model of electron density we have taken tabular profile. For the purpose of HF OTH Radar, the electron density distribution of D, E and F regions is required. The studies of different regions have been carried out by different workers. The data used in this work for electron density is given in table 4.1.[5, 12] and plotted at Fig. 4.1.

Height in Km	Electron Density Distribution High solar act.day in electrons cm^{-3}	Low solar act. day in electron. cm^{-3}	High solar act. Night. in electrons cm^{-3}
60.0	1.00×10^{1}	1.25×10^{1}	1.00×10^{-2}
70.0	3.49×10^{2}	2.72×10^{2}	1.50
80.0	1.34×10^{3}	9.90×10^{2}	8.40×10^{1}
90.0	1.32×10^{4}	5.54×10^{3}	1.90×10^{3}
100.0	6.27×10^{4}	1.74×10^{4}	2.00×10^{3}
110.0	2.00×10^{5}	9.00×10^{4}	2.50×10^{3}
120.0	3.00×10^{5}	1.15×10^{5}	2.00×10^{3}
130.0	2.50×10^{5}	7.00×10^{4}	4.00×10^{3}
140.0	3.00×10^{5}	1.00×10^{5}	2.50×10^{3}
150.0	4.00×10^{5}	1.50×10^{5}	7.00×10^{3}
160.0	5.00×10^{5}	2.00×10^{5}	2.50×10^{3}
170.0	6.00×10^{5}	1.50×10^{5}	1.50×10^{4}
180.0	6.50×10^{5}	1.10×10^{5}	2.00×10^{4}
190.0	6.70×10^{5}	2.00×10^{5}	1.50×10^{4}
200.0	6.90×10^{5}	2.00×10^{5}	1.50×10^{4}
210.0	7.00×10^{5}	2.00×10^{5}	1.50×10^{4}
220.0	7.20×10^{5}	2.00×10^{5}	1.50×10^{4}
230.0	7.40×10^{5}	2.00×10^{5}	1.50×10^{4}

Table 4.1
Electron Density Distribution

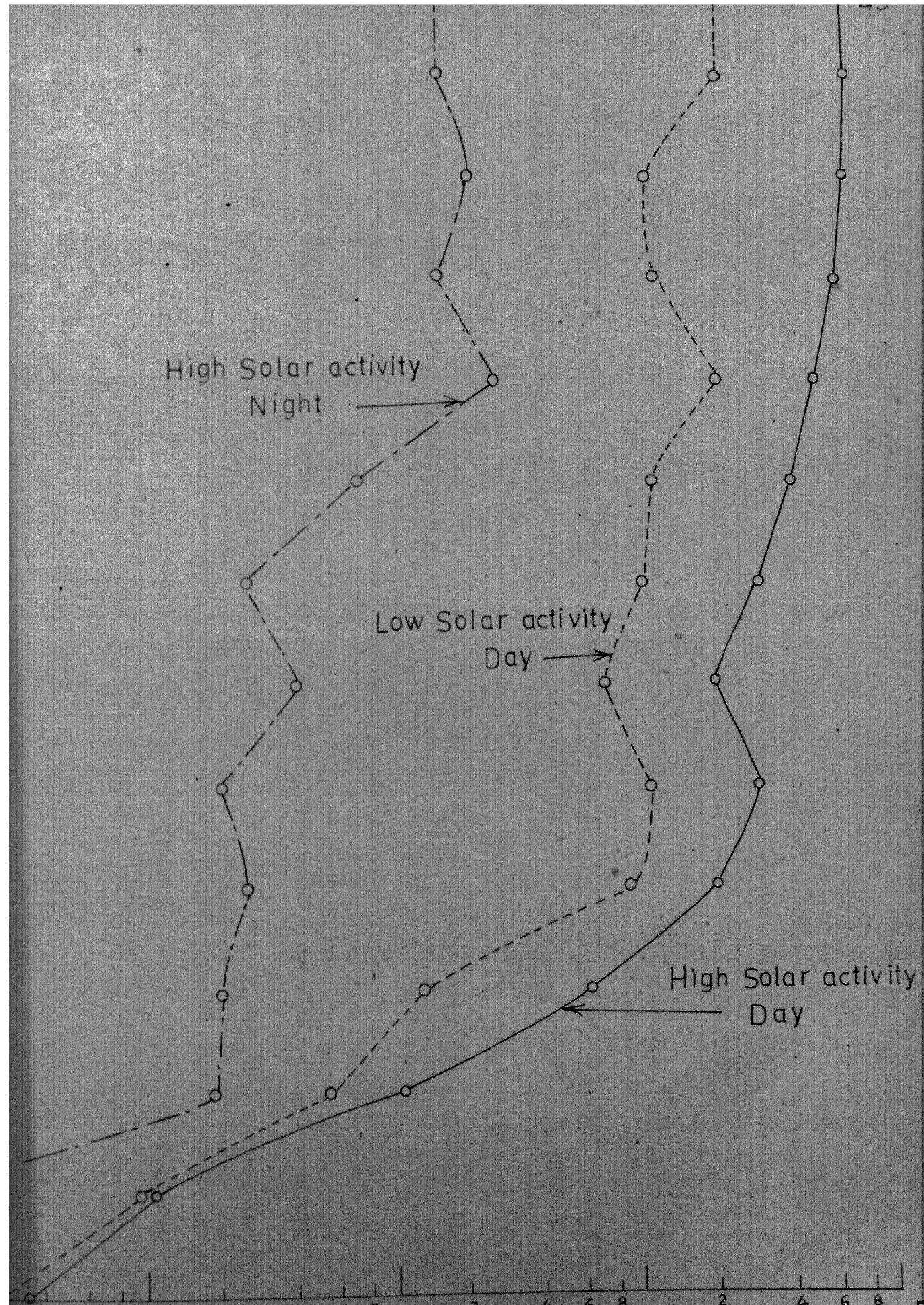
High Solar activity
Night
Low Solar activity
Day
High Solar activity
Day

The data given above is from three different sources as from single source the data for complete height range (60.00 - 230.00 Km) for the different solar activities and time of day were not available. Since we are working with the proposed location of HF OTH Radar at Kanpur (26.5°N, 80.0° E) we have taken the data for mid-latitudes for complete height range and all the three cases of High solar activity, Low solar activity and night time. The details of data from different sources are in following sub-sections.

Data for 60 to 100 Km height above the surface of earth for low and high solar activity, have been taken from the theoritical models of electron density profile under different conditions, , worked out by Chakraborty and Mitra.[5] These data are as a result of a ionochemical scheme given by Mitra and Rowe. The data for night time have been taken only for 70 and 80 Km from Chakraborty and Mitra and above 90 Km in this case is experimental data by Smith L.G. et.al. [23].

Data for Height 100 to 230 Km above the surface of earth is out of experimental measurements by different authors. For solar activity High and Low is from the results quouted by Hirao [13]. This is abtained mainly with rocket probe and some by ground based radio

equipment. The data has been taken from the available curves. The data for night time electron density is also for nearly solar maximum year. It is taken with the help of Langmuir probe and Geiger counter fitted in Nike Apache 14.439 on 1 Nov.72 which was the disturbed night with magnetic-storm.

Thus we have the data for extreme possible ionospheres. The values of ionospheric effects calculated with this data when used in design of HF OTH radar will give the realistic assessment of the capabilities of radar equipment. Also the radar would work for any ionosphere in mid-latitude region with reliability.

4.2.2 Ionospheric Irregularity Model[3, 13, 14]: The irregularity model used is a toroidal model lying in east-west direction. The cross section of the irregularity is assumed to be elliptical in shape. The electron density of the ionosphere with the irregularity present can now be written as

$$N = N_o \left[1 + \Delta(r, \theta) \right] \qquad (4.7)$$

where

N = electron density including the irregularity.

N_o = electron density without the irregularity (given by tabulated model at section 4.2.1.

(r, θ) = electron density of irregularity.

If we take that the electron density is assumed to have the Gausian distribution in the irregularity then we have

$$\Delta(r,\theta) = Co\ Exp\left[-\left\{\frac{(a+Ho)(\theta-\pi/2+\lambda)\cos\beta+(R-a+Ho)\sin\beta}{A}\right\}^2 - \left\{\frac{(R-a-Ho)\cos\beta-(Ro+Ho)(\theta-\pi/2+\lambda)\sin\beta}{B}\right\}^2\right] \quad (4.8)$$

where

Co = amplitude of the irregularity at the centre

a = radius of earth

R, , θ = position of the centre of the cros-section of irregularity in spherical polar coordinates.

A = Semi-Major axis of ellipse in Km.

B = Semi-Minor axis of ellipse in Km.

β = The tilt of an ellipse.

Ho = The height of the irregularity above ground.

λ = The geomagnetic latitude of irregularity.

For the purpose of the work reported in this thesis irregularity data, as given in table 4.2 below.(These are the experimental results discussed in section 3.4 earlier) have been used.

Ho in Km	A in Km	B in Km	Co in electron cm^3	ψ in deg.	Velocity V in Km/sec
100					
	80.0	10.0	.1	-15°	.2
150					

Table 4.2

Irregularity data (the symbols have the meaning given earlier).

4.2.3 Collision Frequency Model and data [3 13 20]: The collision frequency, used here, is in tabular model. This gives more realistic values of collision frequencies instead of a constant collision frequency model. The data have been taken from the work of Shkarofsky [20], which is in agreement with experimental observations of number of scientist, referred by him. Shkarofsky has plotted the results of collision frequency along with the experimental values obtained with Rocket and sputnik III. His results are based on the theoritical studies.

The data used is listed below in table 4.3.

4.3.

Height (Km) above ground	Collision Frequency in Hz
60.0	20.89×10^6
70.0	50.12×10^5
80.0	85.11×10^4
90.0	97.72×10^3
100.0	15.85×10^3
110.0	7.94×10^3
120.0	4.00×10^3
130.0	3.00×10^3
140.0	2.50×10^3
150.0	2.50×10^3
160.0	2.50×10^3
170.0	2.50×10^3
180.0	2.50×10^3
190.0	2.50×10^3
200.0	2.50×10^3
210.0	2.50×10^3
220.0	2.50×10^3
230.0	2.50×10^3

Table 4.3

'Electron collision frequencies'

4.3 Radar Ray Path Results:

The ray path, for azimuthal sweep of 60° (345° to 045°) and for elevation angles from 0 degrees to 5 degrees and frequency 2 to 20 MHz, has been computed with three dimensional ray tracing program electron density and collision frequency has been taken as given at tables 4.1 & 4.3. The effect of magnetic field has been neglected in all computations. The model of irregularity is assumed to have no longitudinal dependence(Toroidal irregularity is taken). The ground range is the one way range of radar signal and not the radar range in usual sense of the usage of the word in conventional radars. Similarly all the parameters computed, viz., ionospheric absorption and doppler shift are also for one way path only. This has been done since the HF radar may have transmitter at one location and receiver at different location (3000 Km from transmitter). However, this being a ground radar equipment we have assumed transmitter and receiver both on ground as far as their antenna heights are concerned . The location of the transmitter is Kanpur (Lat.26.5°N , long. 80° E). The 60° azimuthal coverage (345° to 045°) and 5° vertical beam width (0° to 5° elevation) has been considered. The representative figures of the results of the computation are tabulated in tables

4.4 to 4.9 and plotted in figures 4.3 to 4.7. The results of particular interest are discussed in detail in the following sections.

4.4 Radar Frequency and Range:

The one way ground range of radar signal has been computed for transmission in elevation angles 0° and 5° in the azimuthal direction 345°, 0° (south to north) and 45 degrees. The results have been tabulated at tables 4.4 through 4.6 and plotted in figures 4.3 through 4.5. The one way ground ranges shows following typical features with the variation of the frequency of propogation:

- The ground range increase with the increase in frequency but for the exception at 11 to 13 MHz during day time of high solar activity period. There is a sharp increase in the range at 11 MHz compared to 10 MHz and below followed by a decrease at 11 MHz (Fig. 4.3). This may be because the ray is trapped between two layer of electron density and travels longer distance before the refractive index becomes zero for reflection to take place.
- The ground coverage for a beam of 5° width (in vertical plane) varies from frequency to frequency. It is 410 Km at 2 MHz and 1075 Km at 19 MHz. The coverage of the

radar is from 529 Km to 3359 Km for a frequency sweep of 2 MHz to 19 MHz for an ionosphere without irregularity whereas the coverage is 669 Km to 3653 Km for the frequency sweep of 2 MHz to 19 MHz. (Fig. 4.3) with irregularity.

- The frequencies above 20 MHz penetrate into the ionosphere for all angles of elevation in case of our ionospheric model.
- The ground range changes with azimuth (Fig. 4.4) if there is irregularity in the ionosphere.
- The maximum usable frequencies for day are 19 MHz and 7 MHz during high and low solar activity and 6 MHz at night for high solar activity. The range, in common zone of transmission frequencies (2-6 MHz) is more during night compared to day and also more during low solar activity compared to high solar activity (Fig. 4.5).
- The irregularity changes the range. It decreases the range in majority of cases (Fig. 4.4) at the assumed positions (hight 115 Km, latitude 32 degrees north and longitude 80 degrees east).
- The skip distances are 940 Km, 1001Km and 1440 Km for the high and low solar activity day and high solar activity night respectively.

Frequency in MHz	Ground Range in Km.			
	Without irregularity		With irregularity	
	45 Azimuth 0° elevation	0° Azimuth 5° elevation	45° Azimuth 0° elevation	0° Azimuth 5° elevation
2	940	529	940	-
3	1070	673	1069	669
4	1079	679	1078	678
5	1097	698	1097	695
6.	1120	719	1118	716
7	1147	748	1144	742
8	1184	784	1175	774
9	1219	820	1210	811
10	1262	873	1246	848
11	1687	1195	1297	912
12	1603	1178	1704	1232
13	1617	1209	1653	1223
14	1661	1256	1667	1260
15	1710	1308	1710	1308
16	1766	1359	1763	1363
17	1815	1421	1816	1415
18	1904	1600	1872	1555
19	2284	3359	2025	3653
20	penetrates into the ionosphere			

Table 4.4

Showing Ground Range and Frequency changes with irregularity and without irregularity in ionosphere during day for

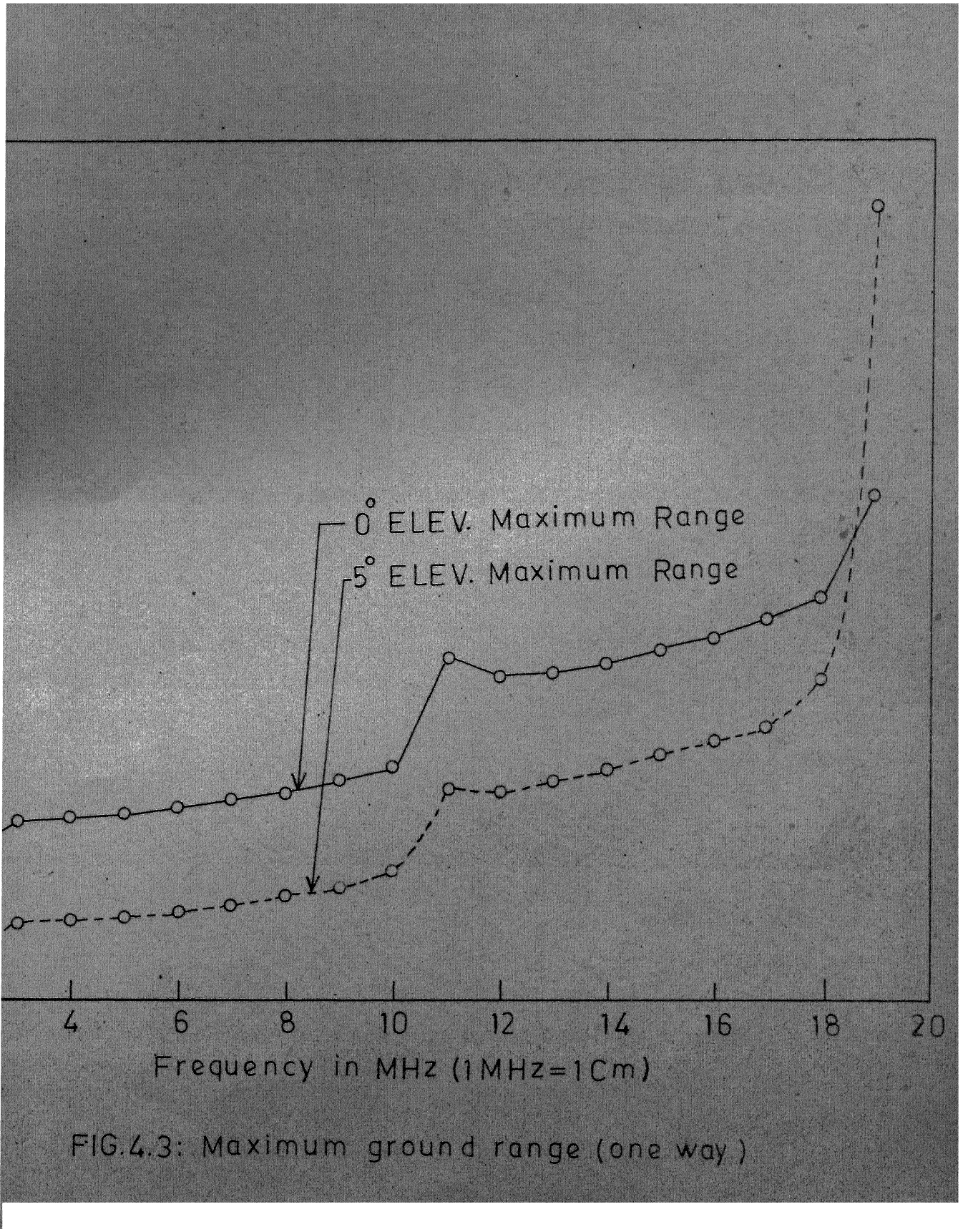

FIG.4.3: Maximum ground range (one way)

quency MHz	Ground Range in Km dt 0° elevation ·			
	0° Azimuth with and without irregularity	45° Azimuth with irregularity	without irregularity	with & without irregularity
2	-	-	-	-
3	1070	1069	1070	1070
4	1079	1078	1079	1079
5	1097	1097	1097	1097
6	1120	1118	1121	1121
7	1147	1144	1147	1147
8	1184	1175	1184	1184
9	1218	1210	1218	1218
0	1262	1246	1262	1262
1	1701	1297	1687	1701
2	1603	1704	1603	1603
3	1617	1653	1617	1617
4	1661	1667	1661	1661
5	1710	1710	1710	1710
6	1765	1763	1765	1765
7	1815	1816	1815	1815
8	1904	1872	1904	1904
9	2282	2025	2282	2282
0	It escapes into the ionosphere			

Table 4.5

Azimuth variation of ground range with irregularity perturbation
(H+ 115 Km, Lat. 32 deg N).

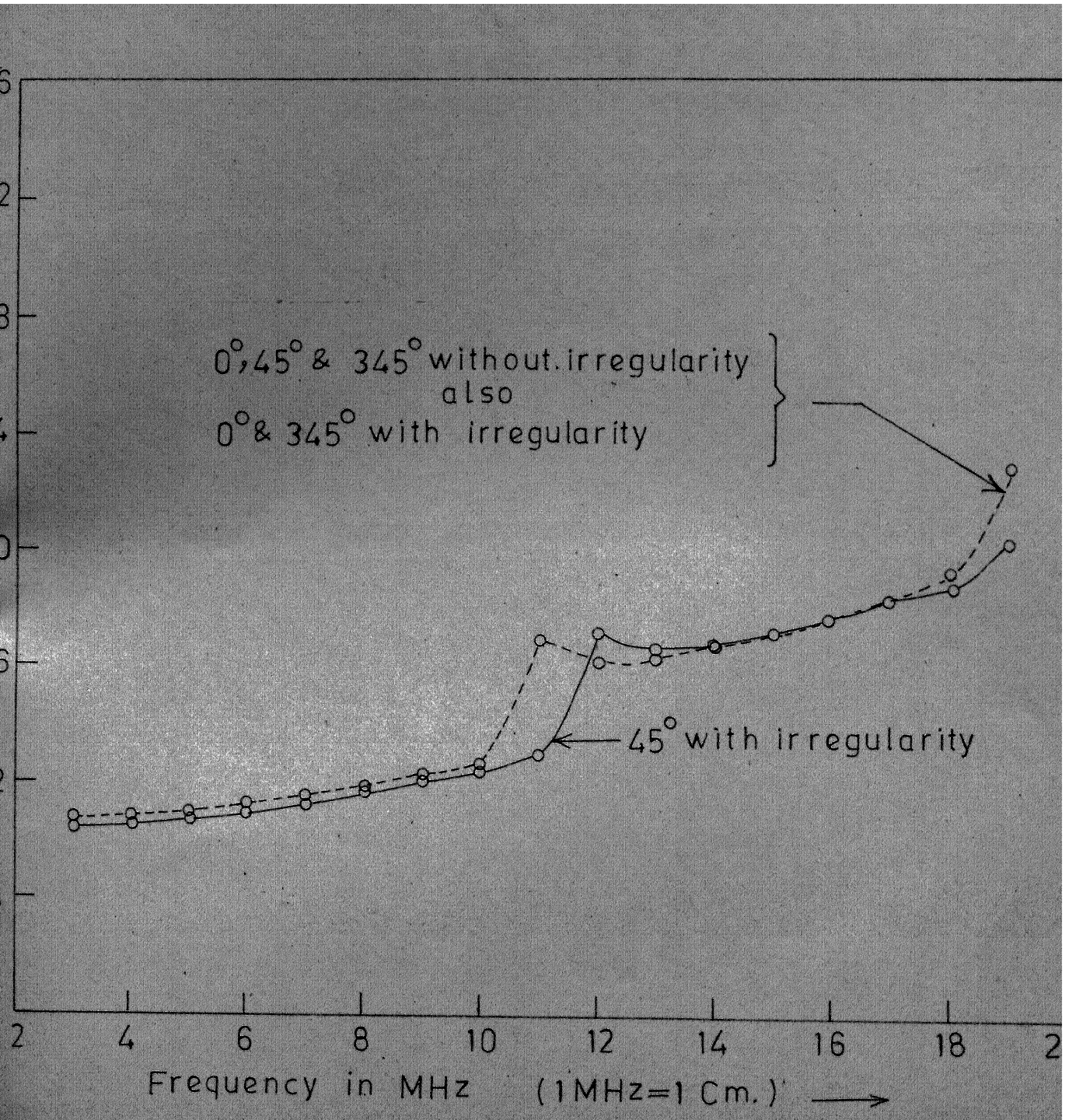

FIG.4·4: Azimuthal variation of range with irregularity

Frequency in MHz	Maximum Range in Km		
	Day High solar	Day Low solar	Night High solar
2	940	1001	1440
3	1069	1081	1514
4	1079	1103	1584
5	1118	1164	1659
6	1144	1425	1762
7	1149	1438	
8	1175		
9	1210		
10	1246		
11	1297		
12	1704		
13	1653		
14	1667		
15	1710		
16	1763		
17	1816		
18	1872		
19	2025		
20	-		

Table 4.6

'Maximum range for High & Low solar activity with diurnal variation'.

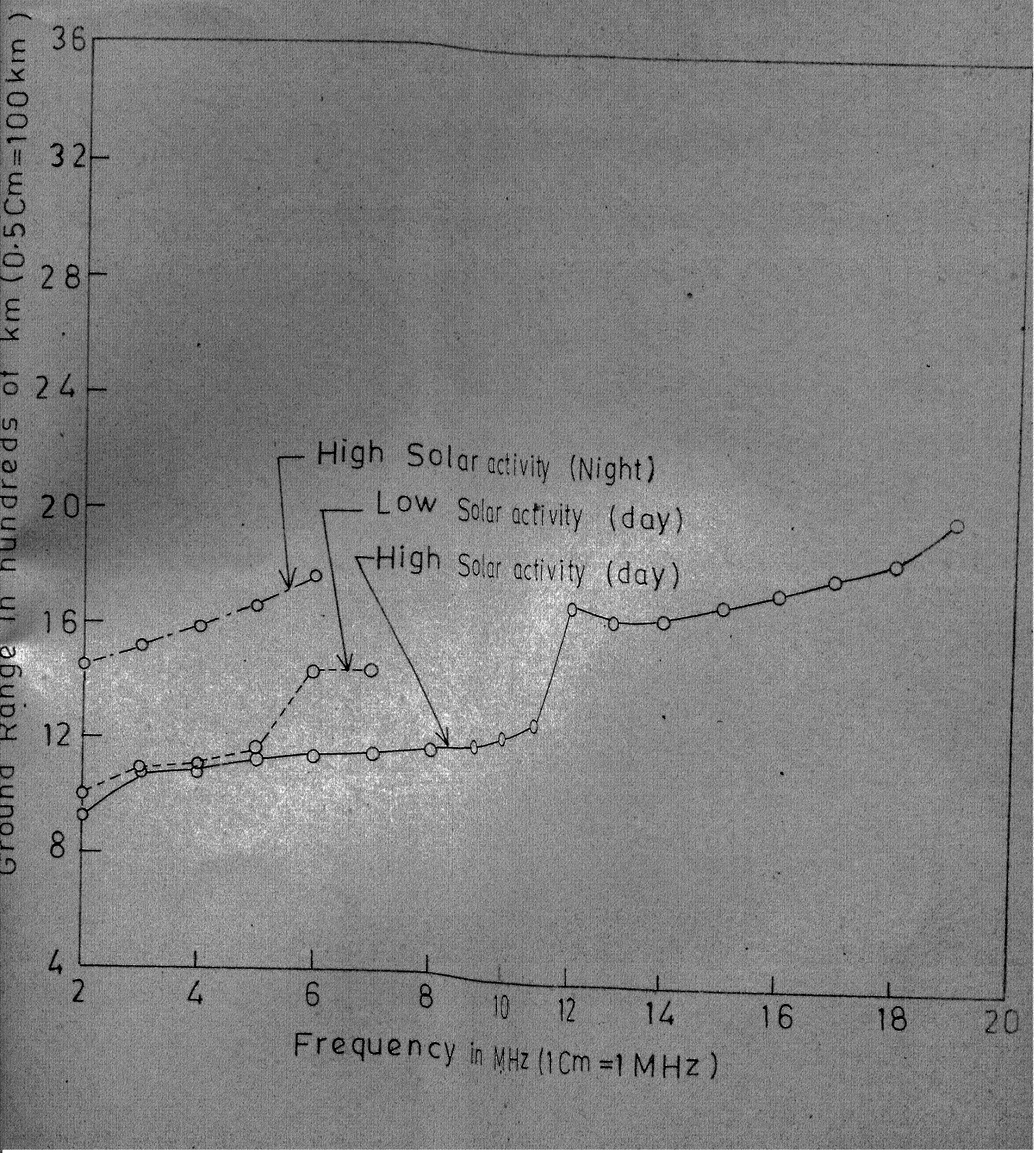
Ground Range in hundreds of km (0.5Cm=100km)
36
32
28
24
20
16
12
8
4
High Solar activity (Night)
Low Solar activity (day)
High Solar activity (day)
2
4
6
8
10
12
14
16
18
20
Frequency in MHz (1Cm =1 MHz)

Frequency in MHz	Absorption in Decibels					
	Day		Day		Daynight	
	High solar		Low solar		High solar	
	No irrty.	irrty.	No irrty.	with irrty.	No irrty.	with irrty
2	-	-	37.1	37.4	7.5	8.4
3	19.1	19.1	14.5	14.5	3.8	4.1
4	11.9	12.0	9.8	9.8	2.4	2.5
5	8.4	8.5	8.9	9.5	1.7	1.8
6	6.7	6.0	8.0	8.3	1.4	1.4
7	5.9	5.7	6.4	6.5		
8	5.5	5.3				
9	5.1	4.9				
10	4.8	4.5				
11	7.8	4.4				
12	5.6	6.6				
13	4.9	5.2				
14	4.5	4.5				
15	4.3	4.2				
16	4.1	4.0				
17	4.0	3.9				
18	4.1	3.8				
19	5.8	4.3				
20	-					

Table 4.7

Maximum absorption in any direction in azimuth sector 345° to 045° with irregularity-(Ht. 115 Km & Lat. 32.0° N) and without irregularity at elevation mentioned in column.

- The maximum ranges acheivable during day with high and low solar activity and during night of high solar activity are 3653 Km, 1438 Km and 1762 Km respectively (Fig. 4.3 and 4.5).

4.3 Ionospheric Absorption:

The ionospheric absorption has been calculated for frequency range 2 MHz through 19 MHz for elevation angles 0 degrees and 5 degrees. The results are at table 4.7 and their plots at figure 4.6. It reveals that;

- The ionospheric absorption decreases with the increase in frequency of transmission.
- The absorption during night is different than during day. It is higher for low solar activity compared to high solar activity.
- The variation of absorption are similar to those of range (11 MH to 13 MHz) during high solar activity.
- The very high value of absorption during low solar activity day may be due to the ray progating in 'D' region where collision frequency is very high and hence more loss of

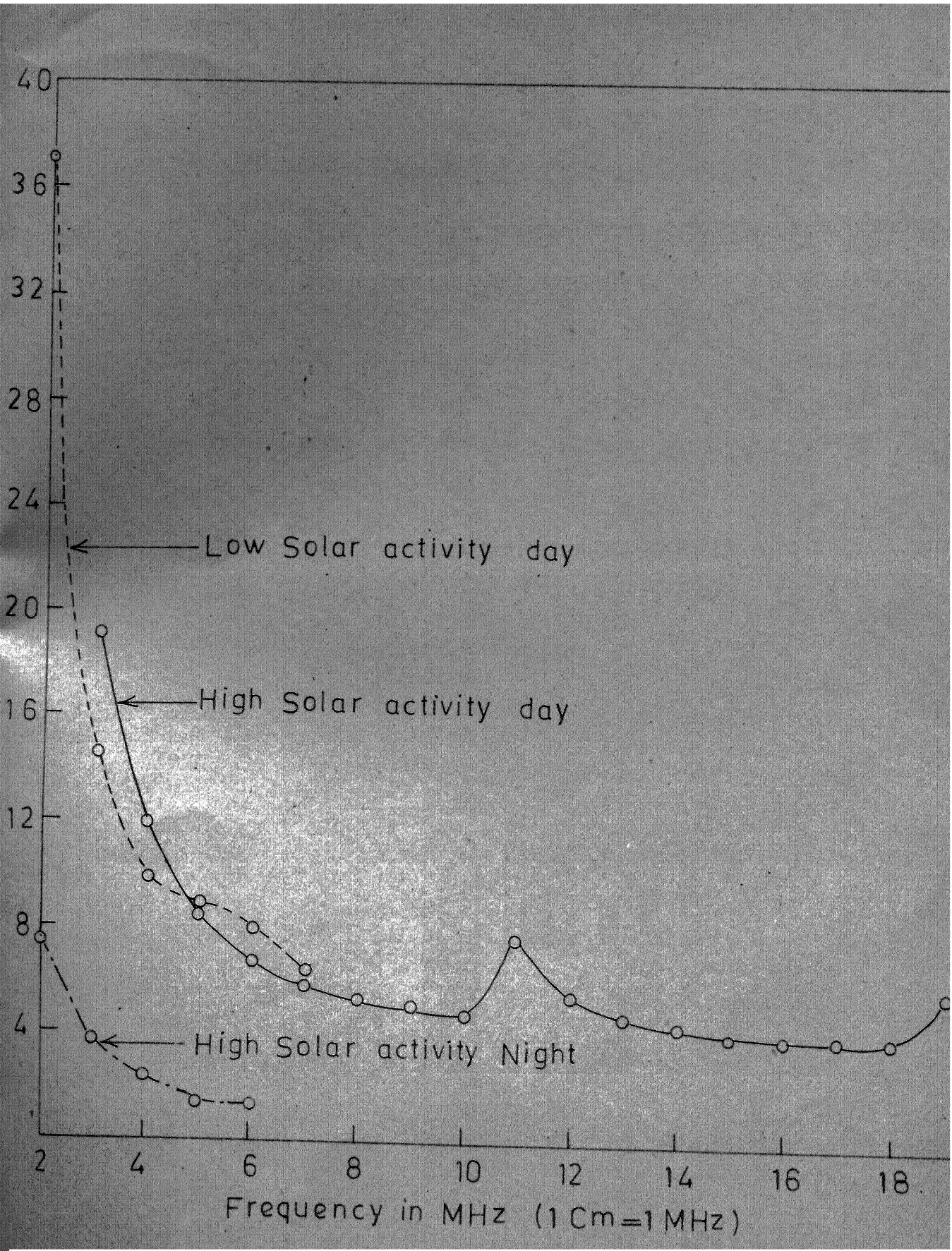
40
36
32
28
24
20
16
12
8
4
Low Solar activity day
High Solar activity day
High Solar activity Night
2
4
6
8
10
12
14
16
18
Frequency in MHz (1 Cm = 1 MHz)

4.3 Ionospheric Doppler Shift:

The ionospheric doppler shift is given by (3.32).

$$\Delta f = \frac{K}{2\mu\mu' fc} \int_{P'} \left(-\frac{1}{r}\right) \frac{dN}{d\lambda} V \, dP'$$

$\frac{dN}{d\lambda}$ is obtained from the toroidal profile of electron density irregularity, which we have chosen for the purpose of this work. Let the electron density of ionosphere with irregularity be given by (as in eqn. 4.7)

$$N(r, \theta, \phi) = No\ (1 + \Delta(r, \theta, \phi)$$

Differentiating (4.7) w.r.t λ we get

$$\frac{dN}{d\lambda} = No \frac{d}{d\lambda} (\Delta(r, \theta, \phi))$$

$$= -2\Delta(r,\theta,\phi)\ (a + Ho)\left(\frac{R\cos\beta}{A^2} - \frac{Y\sin\beta}{B^2}\right) \qquad (4.9)$$

Thus we can rewrite 3.32 as

$$\Delta f = \frac{K}{2\mu\mu' fc} \int_{P'} V.2\ (a+Ho)\,\Delta(r,\theta,\phi)\ \frac{No}{r}\left(\frac{P\cos\beta}{A^2} - \frac{Y\sin\beta}{B^2}\right) dP' \qquad (4.10)$$

where

$$P \triangleq (a+Ho)(\theta - \pi/2 + \lambda)\cos\beta + (r-a-Ho)\sin\beta$$

$$Y \triangleq (r-a-Ho)\cos\beta - (\theta - \pi/2 + \lambda)\sin\beta$$

diff. (4.10) we get

$$\frac{d}{dP}(\Delta f) = \frac{K}{2\mu\mu' f c}\frac{No}{r}(a+Ho)\left(\frac{P\cos\beta}{A^2} - \frac{Y\sin\beta}{B^2}\right)V\Delta(r,\theta) \qquad (4.11)$$

The computation of doppler shift made with the help of ray tracing program are placed at table 4.8. The irregularity has been assumed to be at 115 Km height at 32 degrees latitude. It has a speed of 200 meters/sec. The results of doppler shift show that:

- The doppler shift is always present in any ionospheric (day, night & high/low solar activity) propogation (Fig. 4.7).
- The doppler shift is always less than 1 Hz for 200 M/sec velocity of irregularity (table 4.8).
- The doppler shift is lowest for the propogation during night

The computation were also made for doppler shifts at other heights, latitudes and velocities. The maximum doppler sh was 1.5Hz with 2Km/sec. speed of irregularity. These figures are in agreement with the figures reported by Skolnik[22] and Headricks[12].

Frequency in MHz	Max. Doppler shift in Hz		
	High solar activity day elevation 0 to 5 Degs.	Low solar activity day 0 Deg. to 5 Degs.	High solar activity night 0 Deg. to 5 Degs.
2	-	+ .002	- .008
3	- .017	+ .020	- .004
4	- .022	+ .040	- .002
5	- .030	+ .087	- .001
6	- .041	+ .046	- .000
7	- .054	+ .035	
8	- .006		
9.	- .072		
10	- .078		
11	- .086		
12	- .106		
13	- .123		
14	- .117		
15	- .106		
16	- .093		
17	- .081		
18	- .070		
19	- .060		
20	- .		

Table 4.8

Maximum doppler shift for an irregularity (80.0x10.0 Km elliptical cross section) at 115 Km above ground with 200 Meters/sec speed in Azimuth sector of 345° to 45°.

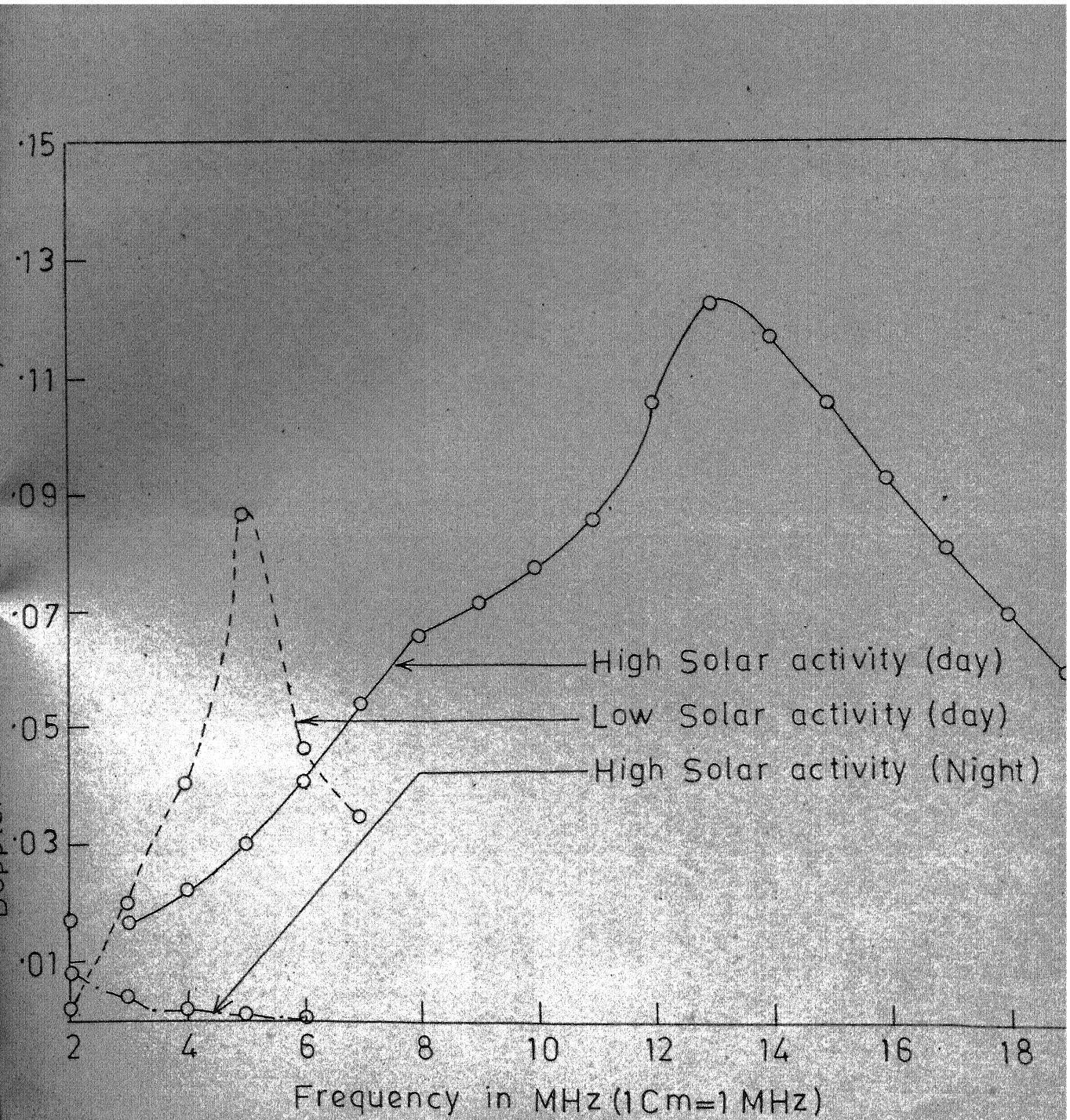

FIG. 4.7: Doppler shift due to an irregularity

The interpolations of group-path differences for perturbed and unperturbed ionosphere show that the maximum error in the range measurement are of the order of ± 48 Km except for the unusal behaviour at 10 to 12 MHz range and at the maximum range of 3359 Km where the errors in range measurement could be as high as ± 300 Km (table 4.9).

Frequency in MHz	Group-path change in Km due to perturbation at 0°	Group-path change in Km due to perturbation at 5° elevation
2	0	-4
3	-2	-4
4	-2	-2
5	0	-4
6	-3	-5
7	-5	-7
8	-9	-13
9	-12	-12
10	-18	-68
11	-402	-295
12	-98	+ 43
13	+32	+ 19
14	+ 1	+ 1
15	- 5	- 2
16	- 7	+ 2
17	- 3	- 7
18	-34	-48
19	-273	+308

Table 4.9

Group-path changes due to irregularity

CHAPTER 5

CONCLUSIONS

The ionospheric effects on the radar signal have been studied with the help of three dimensional ray tracing program. The simulation of ground radar was for 60° azimuthal sweep and 5° in vertical beam width. The detailed study has been in respect of following parameters.

(a) Variation of ground range with frequency.

(b) The coverage of ground range by a 5° beamwidth in vertical plane.

(c) Maximum and minimum range achievable with the assumed profile of electron density.

(d) Ionospheric absorption sufferred by the signal due to collisions of electrons with other particles.

(e) Doppler-shift of the signal due to irregularities in its path.

(f) Group-path difference due to irregularity in ionosphere.

In addition we have made computation of doppler shift for the 2 Km/sec. velocity of the irregularity and absorption for constant collision frequency model.

The conclusion drawn, as a result of this study are given below.

1. The ground range (one way path)increases with the increase of frequency.

2. The ground range shows significant change in the frequency range 10-13 MHz and this produces large group-path difference. This results in unreliable range measurements at these frequencies for our electron density profile.

3. The ground range varies in different directions due to the irregularities present in the ionosphere.

4. The ground coverage also varies due to the irregularities (perturbation).

5. The absorption of the radar signal decreases with the increase in frequency of transmission.

6. The absorption varies due to the presence of irregularities.

7. The absorption at the same frequency varies diurnally and with the solar activity. It being minimum at night time and maximum during low solar activity.

8. The doppler-shift is less than 1 Hz under all conditions for an irregularity of 200 M/sec velocity along the north-south direction.

9. Doppler frequency varies due to the azimuthal rotation and vertical movement of radar beam.

10. Doppler shift is maximum in the middle of frequency spectrum (2 to 19 MHz) being considered.

11. The most suitable frequency range would be 5 MHz to 18 MHz.

The study of ionospheric effects can be made realistic with the detailed and practical ionospheric electron density models for the geographical locations of interest with diurnal and solar cycle variations. More appropriate method would be to have a separate ionospheric sounding radar along with the HF O.T.H. radar to give real-time ionospheric electron density to cater for optimum frequency of operation for the desired range and ground coverage. This would make the design of O.T.H. radar a costly proposal but the advantages of it would always outweigh the cost factor.

REFERENCES

1. Barrick, D.E., et.al; 'Sea back-scatter at H.F.: Interpretation and utilization of the echo' Proc.IEEE vol. 62, No. 6, June 74, pp. 673-80.

2. Bailey D.K., 'The effect of Multipath Distortion on the Choice of Operating Frequencies for H.F. Communication Circuits. IRE Trans. on A&P vol. AP-7, 1959 pp. 379-404.

3. Bain W.C. & Harrison M.D., 'Model Ionosphere for D region at summer noon during sun-spot maximum' Proceedings of the IEE (London) vol. 119 pp. 790-796.

4. Budden, K.G., 'Radio Waves in ionosphere',Cambridge University Press, New York, 1966.

5. Chakrabarty D.K. & Mitra A.P. 'Theoretical Models of D region electron density profiles under different condition'. Indian Journal of Radio & Space Physics vol. 3, 1974 pp. 76-86.

6. Clarke, J. 'Aperture-Synthesis Technique for H.F. Ionospheric Radar' Proc. IEE vol. 117, No. 8, Aug. 70, pp. 1633-38.

7. Davies, Kenneth, 'Ionospheric Radio Waves, Blaisdell Publishing Company, University of COLORADO, 1968.

8. Davies, Kenneth, 'Ionospheric Radio Propogation, Dover publication, Inc. New York, 1966.

9. Gething P.J.D., 'Relationship between oblique and grand path-lengths in ionospheric propogation over a curved earth, 'Nature, London 193, 260, 1962.

10. Gething P.J.D., 'Relationship between phase path and effective path for oblique ionospheric propogation, J. atom. terr. phys., 27, 57, 1965.

11. Harish Chandra et.al. 'Ionospheric irregularities and their Drifts at Thumba during 64-68' Indian Journal of Pure and Applied Physics vol. 8, September,1970, pp. 548-550.

12. Headrick, J.M. & Skolnik, M.I., 'O.T.H. Radar in H.F. band', Proc. IEEE vol. 62, No. 6, pp. 644-672, June, 1974.

13. Hirao, K., 'D-region electron Density Profiles in Mid-Latitude Stations', Indian Journal of Radio and Space Physics,vol. 3, March 1974, pp. 109-112.

14. Jones, R.M., 'A three Dimensional Ray tracing Program' ESS A Tech. Report, IER 17-ITSA 17, 1966.

15. Jones, R.M., 'Modifications to the Three-Dimensional Ray tracing Program Described in IER 17-ITSA 17", 1968.

16. Jordan, E.C. 'Electromagnetic Waves & Radiating Systems', Prentice Hall, 1969.

17. Pandey, R.P., 'Ray tracing study of ionospheric effects on H.F. and V.H.F. Radio Waves', M.Tech. Thesis Deptt. of E.E. , I.I.T. Kanpur, 1974.

18. Peter Laurie, 'An eye on the enemy over the horizon' New Scientist Vol. 64, pp. 420.

19. Satya Prakash et.al. 'A review of the in-situ measurements of E-region irregularities' PRL Ahmedabad Report.

20. Shkarofsky, I.P., ' Generalized Ap Appleton-Hartee equation for any degree of ionisation and Application to the Ionosphere' Proceedings of I.R.E. vol. 49, pp. 1857-1871, Dec. 1961.

21. Singh, Sarabjit, 'Computerised Three dimensional ray tracing in the ionosphere, M.Tech. Thesis Department of E.E. Indian Institute of Technology, Kanpur, 1972.

22. Skolnik M.I., 'Introduction to Radio Systems' McGraw-Hill, Inc.

23. Smith L.G. et.al. 'Energetic electrons in the Mid-latitude Journal of Atmospheric and Terrestrial Physics, 1974 vol. 36, pp. 1601-1612.

24. Srivastava & Tantry, 'Study of irregularities in the F-region of the ionosphere' Indian Journal of Pure and Applied Physics, vol. 8, Sep. 70, pp.560-63.

25. Titheridge, J.E., 'Large-scale Irregularities in the Ionosphere' Journal of Geophysics Research, vol. 68, No. 11 pp 3399-3417, 1963.

26. Titheridge, J.E. 'The Characteristics of Large ionospheric irregularities' Journal of Atmospheric and terrestrial Physics, 1968, vol. 30, pp. 73-84.

27. Tyagi T.R., et.al. 'Characteristics of large-scale Ionospheric irregularities' Indian Journal of Pure & Applied Physics, vol. 8, Sept. 70, pp. 555-559.

A 47080

Date Slip

This book is to be returned on the date last stamped.

.....	.....
.....	.....
.....	.....
.....	.....
.....	.....
.....	.....
.....	.....
.....	.....
.....	.....
.....	.....
.....	.....

CD 6.72.9